Polarized gluon distribution in the proton from holographic light-front QCD

Bheemsehan Gurjar,[1,*] Chandan Mondal,[2,3,†] and Dipankar Chakrabarti[1,‡]

[1]*Indian Institute of Technology Kanpur, Kanpur-208016, India*
[2]*Institute of Modern Physics, Chinese Academy of Sciences, Lanzhou 730000, China*
[3]*School of Nuclear Science and Technology, University of Chinese Academy of Sciences, Beijing 100049, China*

(Received 3 October 2022; accepted 21 February 2023; published 9 March 2023)

We obtain the gluon parton distribution functions (PDFs) in the proton within the extended light-front holographic QCD framework, where the proton couples with the spin-2 Pomeron in anti–de Sitter space, together with constraints imposed by the Veneziano model. The gluon helicity asymmetry, after satisfying the perturbative QCD constraints at small and large longitudinal momentum regions, agrees with existing experimental measurements. The polarized gluon distribution is consistent with global analyses. We predict the gluon helicity contribution to the proton spin, $\Delta G = 0.221^{+0.056}_{-0.044}$, close to the recent analysis with updated datasets and PHENIX measurements and the lattice QCD simulations. We subsequently present the unpolarized and polarized gluon generalized parton distributions in the proton.

DOI: 10.1103/PhysRevD.107.054013

I. INTRODUCTION

How the proton spin emerges from its constituents, quarks and gluons, is one of the key puzzles in modern particle and nuclear physics. In this context, the proton spin decomposition into separate quark and gluon contributions is not unique and is intrinsically debatable due to quark-gluon couplings [1–3]. The well-known proton spin decomposition proposed by Jaffe and Manohar reads [4]

$$\frac{1}{2} = \frac{1}{2}\Delta\Sigma + L_q + L_g + \Delta G, \tag{1}$$

with quark helicity $\frac{1}{2}\Delta\Sigma$, quark orbital angular momentum (OAM) L_q, gluon helicity ΔG, and gluon OAM L_g. The quark and gluon helicity components are related to their polarized parton distribution functions (PDFs), while their OAM contributions are linked to the generalized parton distributions (GPDs) [5–8]. The Jaffe-Manohar decomposition is not the unique way to decompose the proton spin. Ji proposed a frame-independent and gauge-invariant approach for dividing the proton spin into quark helicity, quark OAM, and gluon total angular momentum contributions [9]. On the basis of naive understanding from the quark model, one would expect that the quark spin component contributes the majority of the spin sum rules. However, the famous European Muon Collaboration (EMC) experiment [10] demonstrated that only a tiny portion of the proton spin, $\Delta\Sigma = 0.060(47)(69)$ at $Q^2 = 10\ \mathrm{GeV}^2$ [10,11], is contributed by the quark spin, triggering the problem of the so-called "proton spin puzzle." After a substantial amount of research over the last several decades, it has now been determined that the quark helicity component contributes just around 30% to the proton spin [12–14].

The gluon distributions are extracted less precisely than the quark distributions. However, the accuracy of the extracted unpolarized gluon distribution $g(x)$ has been greatly enhanced over the last decade, and there are still improvements to be made, specifically in the small-x region. In contrast to the unpolarized gluon PDF, the polarized gluon PDF $\Delta g(x)$ is poorly known. It has been shown in Ref. [15] that $\Delta g(x)$ is positive and nonzero in the momentum fraction range $0.05 < x < 0.2$. However, the distribution is quite ambiguous, particularly in the small-x region. For a recent review, see Ref. [16]. Fortunately, the upcoming Electron-Ion Collider (EIC) [17] aims to accurately determine $\Delta g(x)$ at low x and provides rigorous limits on the polarized gluon distribution.

We compute the polarized gluon distribution within the framework based on holographic light-front QCD (HLFQCD) [18] and the generalized Veneziano model [19–21]. HLFQCD is a nonperturbative approach based on the gauge-gravity correspondence [22] and its holographic mapping on light-front QCD [23,24]. A remarkable feature of HLFQCD is that it reproduces the hadronic

*gbheem@iitk.ac.in
†Corresponding author.
mondal@impcas.ac.cn
‡dipankar@iitk.ac.in

spectra with the least number of parameters, the confining strength and the effective quark masses. The effective confining potential for the QCD bound states is uniquely determined by an underlying superconformal algebra [25–27]. HLFQCD generates the structure of hadronic spectra as anticipated by dual models, most notably the Veneziano model [19–21] with its defining characteristics, linear Regge trajectories with a universal slope. This novel approach has been successfully employed to simultaneously derive the quark distributions in the nucleon and the pion [28,29], as well as the strange-antistrange and the charm-anticharm asymmetries in the nucleon [30,31]. Recently, the unpolarized gluon distributions in the nucleon and the pion have also been successfully determined using the universality properties of parton distributions in LFHQCD [32].

We determine the polarized gluon distribution $\Delta g(x)$ and the gluon helicity asymmetry $\Delta g(x)/g(x)$, as well as the gluon GPDs in the proton. One salient issue can be addressed with our study, which concerns the description of the experimental data on the gluon helicity contribution ΔG to the proton spin sum rule [Eq. (1)]. The RHIC spin program at Brookhaven National Laboratory (BNL) [13–15,33,34] and the recent lattice QCD simulations [35] have revealed that $\Delta G = \int_0^1 \mathrm{d}x \Delta g(x)$ is nonvanishing and likely sizable. Several global analyses have been performed to establish limitations on ΔG using various experimental datasets and parametrizations [36–39]. Using updated datasets and PHENIX measurements [40], a recent extraction yielded $\Delta G = 0.2$ with a restriction of $-0.7 < \Delta G < 0.5$ for the gluon momentum fraction $0.02 \leq x \leq 0.3$. It was reported in Ref. [13] that $\Delta G = \int_{0.05}^{0.2} \mathrm{d}x \Delta g(x) = 0.23(6)$, and in Ref. [15] that $\Delta G = \int_{0.05}^{1} \mathrm{d}x \Delta g(x) = 0.19(6)$. Meanwhile, the large-momentum effective theory [41,42] provides $\Delta G(\mu^2 = 10\ \mathrm{GeV}^2) = 0.251(47)(16)$, which is almost half of the proton. In order to confine $\Delta g(x)$ at low x, some theoretical constraints have been discussed in Ref. [43]. Several experiments are now being conducted at the RHIC [44,45], HERMES [46], JLab [47], and COMPASS [48] to obtain high-precision measurements of the gluon helicity ΔG. Addressing this fundamental issue demands a unified framework, such as we demonstrate here, that adequately provides a prediction of the expected data for the gluon helicity from the future experiments.

II. GLUON DISTRIBUTION FUNCTIONS

A. Unpolarized PDF

The unpolarized gluon distribution function can be derived from the HLFQCD expression of its gravitational form factor (GFF) [32]. To compute the gluon GFF for an arbitrary twist-τ Fock state in the light-front Fock expansion of the proton state, $A_\tau^g(t)$, the Pomeron is considered to couple mainly to the constituent gluon [49–53]. The lowest twist is the $\tau = 4$ Fock state $|uudg\rangle$ in the proton containing a dynamical gluon. The Pomeron couples to the dynamical gluon over a distance $\sim 1/\sqrt{\alpha'_P}$, where α'_P defines the slope of the effective Regge trajectory of the Pomeron. In LFHQCD, the GFF $A_\tau^g(t)$ can be expressed in terms of the Euler beta function $B(u, v)$ as [32]

$$A_\tau^g(t) = \frac{1}{N_\tau} B(\tau - 1, 2 - \alpha_P(t)), \tag{2}$$

where $N_\tau = B(\tau - 1, 2 - \alpha_P(0))$, and where

$$\alpha_P(t) = \alpha_P(0) + \alpha'_P t \tag{3}$$

is the effective Regge trajectory of Donnachie and Landshoff's soft pomeron [54] with intercept $\alpha_P(0) \simeq 1.08$, slope $\alpha'_P \simeq 0.25\ \mathrm{GeV}^{-2}$ [55], with $t = -Q^2$ being the square of transferred momentum. Equation (2) has the same structure as a generalization of the Veneziano amplitude [19–21] for a spin-2 current. Note that while writing Eq. (2), only the dilaton profile [56] $e^{\varphi_g(z)} = e^{-\lambda_g z^2}$ with $\lambda_g = 1/4\alpha'_P \simeq 1\ \mathrm{GeV}^2$ describing Pomeron exchange has been considered. This sets the scale when computing the gluon GFFs and GPDs. Pomeron exchange is recognized as the graviton of the dual AdS theory [57–63]. Meanwhile, only the dilaton corresponding to Reggeon exchange, $e^{\varphi_q(z)} = e^{\lambda_q z^2}$ with $\lambda_q = 1/4\alpha'_\rho \simeq (0.5\ \mathrm{GeV})^2$, needs to be assumed when deriving the electromagnetic form factors and quark GPDs [28].

Using the integral representation of the Euler beta function,

$$B(u, v) = B(v, u) = \int_0^1 \mathrm{d}y\, y^{u-1}(1 - y)^{v-1}, \tag{4}$$

where $\Re(u) > 0$ and $\Re(v) > 0$, in Eq. (2), the gluon GFF $A_\tau(t)$ can be recast in the reparametrization invariant form as

$$A_\tau^g(t) = \frac{1}{N_\tau} \int_0^1 \mathrm{d}x\, w'(x) w(x)^{1-\alpha_P(t)} [1 - w(x)]^{\tau-2}, \tag{5}$$

provided that $w(x)$ is a monotonically increasing function and satisfies the constraints $w(0) = 0$, $w(1) = 1$, and $w'(x) \geq 0$ with $x \in [0, 1]$. The reparametrization function $w(x)$ is introduced in Refs. [28,29,32] and is given by

$$w(x) = x^{1-x} e^{-a(1-x)^2}, \tag{6}$$

with the parameter $a = 0.48 \pm 0.04$. The gluon GFF $A_\tau^g(t)$ can also be written as the first moment of the gluon GPD at zero skewness, $H_\tau^g(x, t)$:

$$A_\tau^g(t) = \int_0^1 \mathrm{d}x\, x H_\tau^g(x, t) = \int_0^1 \mathrm{d}x\, x g_\tau(x) e^{tf(x)}, \tag{7}$$

where $g_\tau(x)$ is the collinear unpolarized gluon PDF of twist τ, and $f(x)$ is the profile function. Comparing Eq. (7) with Eq. (5), one can extract both functions, $g_\tau(x)$ and $f(x)$, in terms of the universal reparametrization function $w(x)$:

$$g_\tau(x) = \frac{1}{N_\tau}\frac{w'(x)}{x}[1-w(x)]^{\tau-2}w(x)^{1-\alpha_P(0)}, \tag{8}$$

$$f(x) = \alpha'_P \log\left(\frac{1}{w(x)}\right), \tag{9}$$

with the normalization condition $\int_0^1 dx x g_\tau(x) = 1$. The PDF for the gluon in the proton is written as the sum of contributions from all Fock states—i.e., $g(x) = \sum_\tau c_\tau g_\tau(x)$. Note that we only consider the leading term, $\tau = 4$, and the coefficient $c_{\tau=4} = 0.225 \pm 0.014$ [32] has been determined by using the momentum sum rule,

$$\int_0^1 \mathrm{d}x\, x\left[g(x) + \sum_q q(x)\right] = 1, \tag{10}$$

with the help of quark distributions $q(x)$ at the hadronic scale $\mu^2 \sim 1$ GeV obtained previously within the HLFQCD framework [28].

B. Helicity PDF

Polarized gluon distributions can be evaluated by using Eq. (8), but with different Pomeron Regge trajectory,

$$\Delta g_\tau(x) = \frac{1}{N_\tau}\frac{w'(x)}{x}[1-w(x)]^{\tau-2}w(x)^{1-\tilde{\alpha}_P(0)}, \tag{11}$$

where the Regge trajectory is given by

$$\tilde{\alpha}_P(t) = \tilde{\alpha}_P(0) + \alpha'_P t. \tag{12}$$

Note that the slope of the Regge trajectories is universal, while their intercepts are different for the unpolarized and the polarized gluon distributions. We determine the value of the intercept $\tilde{\alpha}_P(0)$ by requiring the result to fit the experimental data for the gluon asymmetry ratio, $\Delta g(x)/g(x)$, together with the constraints of $\Delta g(x)/g(x)$ at $x \to 1$ and $x \to 0$ [64,65]. In HLFQCD, the gluon helicity asymmetry behaves as

$$\frac{\Delta g_\tau(x)}{g_\tau(x)} = w(x)^{\alpha_P(0)-\tilde{\alpha}_P(0)}, \tag{13}$$

where the exponent, $\alpha_P(0) - \tilde{\alpha}_P(0)$, is the difference between the intercepts of unpolarized and polarized Regge trajectories. Note that any value of $\tilde{\alpha}_P(0) < \alpha_P(0)$ satisfies the pQCD predictions for the helicity asymmetry retention [64,65]. We fix $\tilde{\alpha}_P(0) \equiv 0$–$0.16$ by fitting the helicity asymmetry to the experimental data. At our center value of $\tilde{\alpha}_P(0) = 0.08$, the χ^2 per d.o.f. for the fit is 1.5.

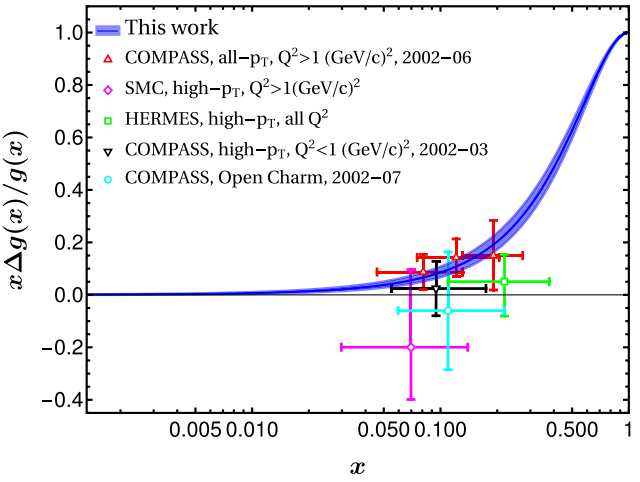

FIG. 1. The gluon helicity asymmetry, $\Delta g(x)/g(x)$, in the proton (blue band) is compared with the available experimental data [66–70]. The direct measurements of COMPASS [66,67], HERMES [70], and SMC [69] are obtained at leading order from high-p_T hadrons, while open charm muon production at COMPASS [68] is taken from next-to-leading order at different values of x. The error band in our result is due to the spread in the Regge intercept $\tilde{\alpha}_P(0) \equiv 0$–$0.16$ and the uncertainties in the parameter $a = 0.48 \pm 0.04$ appearing in the reparametrization function $w(x)$, Eq. (6).

Figure 1 confirms that the gluon helicity asymmetry $\Delta g(x)/g(x)$ satisfies the pQCD constraints at the end points. The helicity asymmetry decreases to zero at small x and increases to one when x approaches 1. The model uncertainty (blue band) includes the uncertainties in the parameter a appearing in the reparametrization function $w(x)$ [Eq. (6)] and the spread in the Regge intercept $\tilde{\alpha}_P(0)$. We compare the ratio $\Delta g(x)/g(x)$ with the data at different gluon longitudinal momentum extracted from high-p_T hadrons in the leading-order analyses [66,67] and from the open charm production in the next-to-leading-order analysis [68] at COMPASS, from high-p_T hadrons at leading-order analyses by the Spin Muon Collaboration (SMC) at CERN [69] and at the HERMES experiment [70]. We find a good agreement between our result and the COMPASS data. Note that there still remain large uncertainties of the ratio $\Delta g(x)/g(x)$, including even the sign from different experiments.

Having specified the gluon helicity asymmetry ratio, we are now in a position to present explicitly the gluon helicity PDF in HLFQCD. We show the intrinsic nonperturbative gluon helicity distribution, $x\Delta g(x)$, defined at the initial scale $\mu^2 \sim 1$ in Fig. 2, where we compare our prediction with the global analyses by the NNPDFpol1.0 [13] and the JAM [71] Collaborations, as well as with other theoretical studies [72–76]. We find a good consistency between our prediction for the proton's gluon helicity PDF and the global fits and the results obtained from various theoretical approaches. The uncertainty band stems from the model

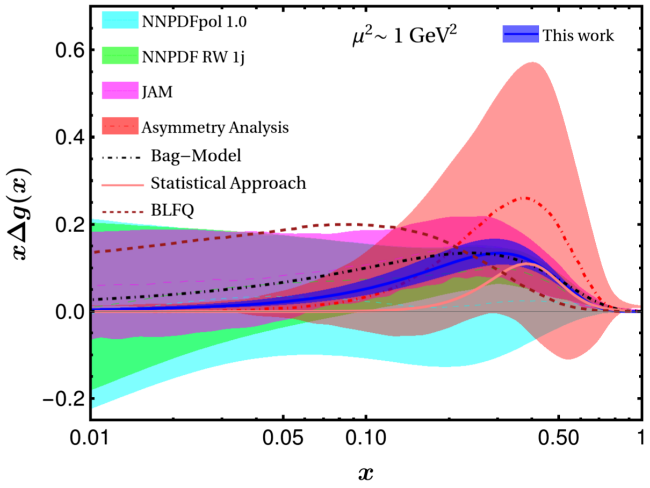

FIG. 2. The polarized gluon distribution $x\Delta g(x)$ at the scale $\mu^2 \sim 1$ GeV^2 (blue band) is compared with the global analyses by the NNPDFpol1.0 [13] (cyan band) Collaboration, the NNPDFpol1.0 reweight RHIC data [13] (green band), and JAM [71] (magenta band), as well as with other theoretical studies: the Bag model [72] (black dash-dotted line), phenomenological fit by the Asymmetry Analysis Collaboration [73] (red dash-dotted line surrounded by an uncertainty band), the statistical approach [74] (pink solid line), and the basis light-front quantization (BLFQ) approach [75] (purple dashed line).

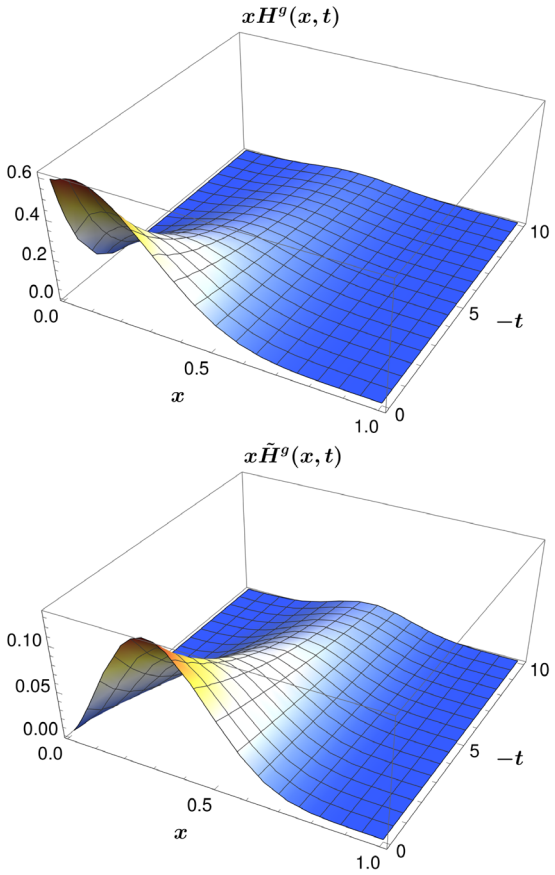

FIG. 3. Three-dimensional structure of the unpolarized (upper panel) and polarized (lower panel) gluon GPDs in the proton as a function of x and $-t$ (in units of GeV^2). These results are generated using the Pomeron exchange with scale parameter $\lambda_g = 1/4\alpha'_P \simeq 1$ GeV^2. The intercepts of the Pomeron trajectories associated with the unpolarized and the polarized GPDs are $\alpha_P(0) = 1.08$ and $\tilde{\alpha}_P(0) = 0.08$, respectively.

parameters, $c_{\tau=4}$, a, and $\tilde{\alpha}_P(0)$. We notice that at the model scale, the percentage uncertainty of $x\Delta g(x)$ is larger than that of $xg(x)$. It should be noted that there are large uncertainties in the global analyses, and thus $\Delta g(x)$ is poorly constrained, including even the sign, especially in the small-x region but also in the large-x region.

The gluon spin contribution ΔG to the proton spin is given by the first moment of the gluon helicity PDF $\Delta g(x)$. Our current analysis predicts that the gluon spin, $\Delta G = 0.221^{+0.056}_{-0.044}$, is sizeable in comparison to the proton spin and close to the recent analysis with updated datasets and PHENIX measurements [40], which yielded $\Delta G = 0.2$ for $x_g \in [0.02, 0.3]$. Excluding the $x_g < 0.05$ region, the values of $\Delta G = 0.23(6)$ for $x_g \in [0.05, 0.2]$ [13] and $\Delta G = 0.19(6)$ for $x_g \in [0.05, 1]$ [15] were reported. For comparison, the lattice QCD calculation at physical pion mass predicts $\Delta G = 0.251(47)(16)$ [35]. Due to the current accuracy of experimentally measured data, the phenomenological extraction of ΔG is sensitive to the parametrization form in the global analyses. One will find large uncertainties of $\Delta g(x)$, and thus very poor constraint on ΔG, if permitting a possible sign change of $\Delta g(x)$ at some values of x [77]. Future measurements of $\Delta g(x)$ in the region $x_g < 0.02$ are necessitated to reduce the uncertainty in ΔG. Resolving this issue is one of the major goals of the future EICs [17,78].

C. Gluon GPDs

Using the expressions of the gluon GFF in Eqs. (5) and (7), we write the unpolarized gluon GPDs at skewness zero in the proton, choosing specific x and t dependences of the GPDs [28] as

$$H^g_\tau(x,t) = g_\tau(x) e^{tf(x)}, \tag{14}$$

where the unpolarized gluon PDF of twist τ $[g_\tau(x)]$ and the universal profile function $[f(x)]$ are given in Eqs. (8) and (9), respectively. In a similar fashion, we express the polarized gluon GPD

$$\tilde{H}^g_\tau(x,t) = \Delta g_\tau(x) e^{tf(x)}, \tag{15}$$

with the polarized gluon PDF defined in Eq. (11). Note that we consider the same t-dependence factor in both the GPDs. This emerges from the linear Regge trajectories associated with the unpolarized and polarized distributions having equal slope. Meanwhile, different intercepts of the trajectories generate different x-dependence structures of those GPDs.

The three-dimensional structures of the gluon GPDs as a function of x and $-t = Q^2 = \vec{q}^2_\perp$ are illustrated in Fig. 3. In the forward limit, $-t = 0$, the GPDs reduce to their

corresponding collinear PDFs. The unpolarized gluon distribution peaks at small x, while the polarized GPD has its peak located at a slightly higher value of x than the unpolarized GPD. The magnitude of $xH^g(x,t)$ is much higher than that of $x\tilde{H}^g(x,t)$. The peaks of these GPDs move toward higher values of x and simultaneously reduce the magnitudes when increasing the value of the momentum transfer $-t$. This seems to be a model-independent behavior of the GPDs, which has also been observed in quark GPDs evaluated within this HLFQCD framework [28], as well as in various phenomenological models for the nucleon [79–89]. As gluon GPDs are not yet experimentally determined, it is not possible to compare our predictions with any data. Nonetheless, the gluon GPDs can be investigated experimentally from deeply virtual Compton scattering (DVCS) and other exclusive processes. The upcoming EICs in the USA [78] and in China [90] can significantly improve our current knowledge of the gluon GPDs. Simulation studies in Ref. [91] show that the proposed high-luminosity EICs can perform accurate measurements of DVCS cross sections and asymmetries in a very fine binning and with a very low statistical uncertainty.

The GPDs in transverse impact parameter space are obtained via the Fourier transform of the GPDs with respect to the momentum transfer along the transverse direction $\vec{q}_\perp$ [92]:

$$\mathcal{F}(x,b_\perp) = \int \frac{\mathrm{d}^2\vec{q}_\perp}{(2\pi)^2} e^{-i\vec{q}_\perp\cdot\vec{b}_\perp} F(x,0,t), \tag{16}$$

with F being the GPDs in momentum space, and $\vec{b}_\perp$ defines the transverse impact parameter conjugate to the transverse momentum transfer $\vec{q}_\perp$. The function $\mathcal{H}^g(x,b_\perp)$ can be interpreted as the number density of gluons with a longitudinal momentum fraction x at a given transverse distance $b_\perp$ in the proton [93]. We can then define the x-dependent squared radius of the gluon density in the transverse plane as [94]

$$\langle b_\perp^2\rangle^g(x) = \frac{\int \mathrm{d}^2\vec{b}_\perp b_\perp^2 \mathcal{H}^g(x,b_\perp)}{\int \mathrm{d}^2\vec{b}_\perp \mathcal{H}^g(x,b_\perp)}, \tag{17}$$

which is uniquely determined by the profile function $f(x)$ [Eq. (9)]. We present the x-dependent squared radius of the proton's gluon distribution in Fig. 4. It shows an increase of the transverse radius with a decreasing value of the gluon momentum fraction x. At large x, the transverse size of the distribution behaves as a pointlike color-singlet object. This nature is the origin of color transparency in nuclei [95]. Note that this behavior is universal and depends only on the profile function $f(x)$, which, in LFHQCD, is determined by the hadron mass scale λ_g and the universal reparametrization function $w(x)$. The general features of $\langle b_\perp^2\rangle^g(x)$ as reported here have also been observed in the dependence of the transverse size of the proton on the quark's longitudinal momentum, which has been determined from DVCS experimental data [94] and investigated in other theoretical studies [88,95].

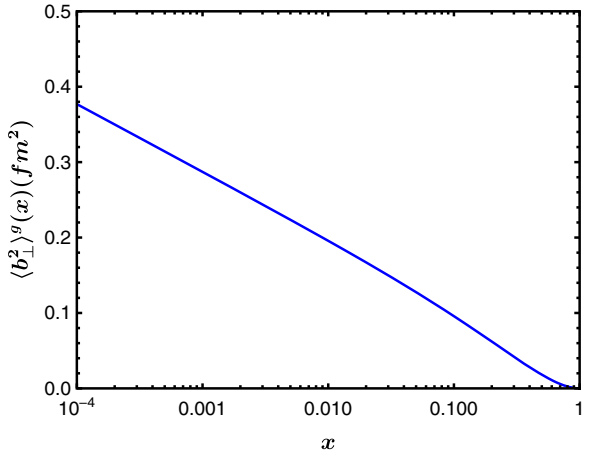

FIG. 4. x dependence of $\langle b_\perp^2\rangle$ for gluons in the proton. This result is obtained using the Pomeron exchange with scale parameter $\lambda_g = 1/4\alpha'_P \simeq 1$ GeV^2.

III. CONCLUSION

We have evaluated the polarized gluon distribution using a unified nonperturbative approach based on the gauge-gravity correspondence, light-front holography and the generalized Veneziano model. The gluon PDFs can be expressed in terms of a universal reparametrization function $w(x)$ [28,29,32]. A simple ansatz for $w(x)$, which satisfies the pQCD constraints for the gluon helicity asymmetry ratio at the end points, $x \to \{0,1\}$, leads to a precise description of gluon helicity distribution. We have observed a good consistency between our prediction for the gluon helicity PDF and the global fits, as well as with the results obtained from various theoretical approaches. The gluon helicity asymmetry ratio is found to be in good agreement with the COMPASS data. Within the HLFQCD framework, we have predicted that at the scale $\mu^2 \sim 1$ GeV^2, the gluon helicity contributes

$$\Delta G = 0.221^{+0.056}_{-0.044}, \tag{18}$$

which is almost 44% of the proton spin. Experimentally, there still remain large uncertainties about the small-x contribution to ΔG. Precise determinations of the gluon helicity distribution in the $x < 0.02$ region are required to constrain ΔG.

We have subsequently presented the unpolarized and polarized gluon GPDs in the proton, choosing specific x and t dependences of the GPDs, using the gluon PDFs and the universal profile function $f(x)$, which can also be expressed in terms of the universal reparametrization function $w(x)$. We have observed that the unpolarized gluon GPD is distinctly different from the gluon-helicity-dependent GPD, whereas the difference between them is given by their corresponding collinear PDFs. We have found that the qualitative behavior of the GPDs in the

HLFQCD approach bears similarities to other phenomenological models.

ACKNOWLEDGMENTS

C. M. is supported by new faculty startup funding by the Institute of Modern Physics, Chinese Academy of Sciences, Grant No. E129952YR0. C. M. also thanks the Chinese Academy of Sciences President's International Fellowship Initiative for the support via Grants No. 2021PM0023. The work of D. C. is supported by the Science and Engineering Research Board under Grant No. CRG/2019/000895.

[1] E. Leader, Phys. Rev. D **105**, 036005 (2022).
[2] M. Wakamatsu, Int. J. Mod. Phys. A **29**, 1430012 (2014).
[3] K.-F. Liu and C. Lorcé, Eur. Phys. J. A **52**, 160 (2016).
[4] R. L. Jaffe and A. Manohar, Nucl. Phys. **B337**, 509 (1990).
[5] X.-D. Ji, Phys. Rev. D **55**, 7114 (1997).
[6] M. Diehl, Phys. Rep. **388**, 41 (2003).
[7] A. V. Belitsky and A. V. Radyushkin, Phys. Rep. **418**, 1 (2005).
[8] K. Goeke, M. V. Polyakov, and M. Vanderhaeghen, Prog. Part. Nucl. Phys. **47**, 401 (2001).
[9] X.-D. Ji, Phys. Rev. Lett. **78**, 610 (1997).
[10] J. Ashman *et al.* (European Muon Collaboration), Phys. Lett. B **206**, 364 (1988).
[11] J. Ashman *et al.* (European Muon Collaboration), Nucl. Phys. **B328**, 1 (1989).
[12] D. de Florian, R. Sassot, M. Stratmann, and W. Vogelsang, Phys. Rev. D **80**, 034030 (2009).
[13] E. R. Nocera, R. D. Ball, S. Forte, G. Ridolfi, and J. Rojo (NNPDF Collaboration), Nucl. Phys. **B887**, 276 (2014).
[14] J. J. Ethier, N. Sato, and W. Melnitchouk, Phys. Rev. Lett. **119**, 132001 (2017).
[15] D. de Florian, R. Sassot, M. Stratmann, and W. Vogelsang, Phys. Rev. Lett. **113**, 012001 (2014).
[16] X. Ji, F. Yuan, and Y. Zhao, Nat. Rev. Phys. **3**, 27 (2021).
[17] A. Accardi *et al.*, Eur. Phys. J. A **52**, 268 (2016).
[18] S. J. Brodsky, G. F. de Teramond, H. G. Dosch, and J. Erlich, Phys. Rep. **584**, 1 (2015).
[19] G. Veneziano, Nuovo Cimento Soc. Ital. Fis. A **57**, 190 (1968).
[20] M. Ademollo and E. Del Giudice, Nuovo Cimento Soc. Ital. Fis. A **63**, 639 (1969).
[21] P. V. Landshoff and J. C. Polkinghorne, Nucl. Phys. **B19**, 432 (1970).
[22] J. M. Maldacena, Adv. Theor. Math. Phys. **2**, 231 (1998).
[23] S. J. Brodsky and G. F. de Teramond, Phys. Rev. Lett. **96**, 201601 (2006).
[24] G. F. de Teramond and S. J. Brodsky, Phys. Rev. Lett. **102**, 081601 (2009).
[25] S. Fubini and E. Rabinovici, Nucl. Phys. **B245**, 17 (1984).
[26] G. F. de Teramond, H. G. Dosch, and S. J. Brodsky, Phys. Rev. D **91**, 045040 (2015).
[27] H. G. Dosch, G. F. de Teramond, and S. J. Brodsky, Phys. Rev. D **91**, 085016 (2015).
[28] G. F. de Teramond, T. Liu, R. S. Sufian, H. G. Dosch, S. J. Brodsky, and A. Deur (HLFHS Collaboration), Phys. Rev. Lett. **120**, 182001 (2018).
[29] T. Liu, R. S. Sufian, G. F. de Téramond, H. G. Dosch, S. J. Brodsky, and A. Deur, Phys. Rev. Lett. **124**, 082003 (2020).
[30] R. S. Sufian, T. Liu, G. F. de Téramond, H. G. Dosch, S. J. Brodsky, A. Deur, M. T. Islam, and B.-Q. Ma, Phys. Rev. D **98**, 114004 (2018).
[31] R. S. Sufian, T. Liu, A. Alexandru, S. J. Brodsky, G. F. de Téramond, H. G. Dosch, T. Draper, K.-F. Liu, and Y.-B. Yang, Phys. Lett. B **808**, 135633 (2020).
[32] G. F. de Téramond, H. G. Dosch, T. Liu, R. S. Sufian, S. J. Brodsky, and A. Deur (HLFHS Collaboration), Phys. Rev. D **104**, 114005 (2021).
[33] L. Adamczyk *et al.* (STAR Collaboration), Phys. Rev. Lett. **115**, 092002 (2015).
[34] M. S. Abdallah *et al.* (STAR Collaboration), Phys. Rev. D **105**, 092011 (2022).
[35] Y.-B. Yang, R. S. Sufian, A. Alexandru, T. Draper, M. J. Glatzmaier, K.-F. Liu, and Y. Zhao, Phys. Rev. Lett. **118**, 102001 (2017).
[36] T. Gehrmann and W. J. Stirling, Phys. Rev. D **53**, 6100 (1996).
[37] M. Gluck, E. Reya, M. Stratmann, and W. Vogelsang, Phys. Rev. D **63**, 094005 (2001).
[38] J. Blumlein and H. Bottcher, Nucl. Phys. **B636**, 225 (2002).
[39] E. Leader, A. V. Sidorov, and D. B. Stamenov, Phys. Rev. D **73**, 034023 (2006).
[40] A. Adare *et al.* (PHENIX Collaboration), Phys. Rev. Lett. **103**, 012003 (2009).
[41] X. Ji, Phys. Rev. Lett. **110**, 262002 (2013).
[42] X. Ji, Sci. China Phys. Mech. Astron. **57**, 1407 (2014).
[43] Y. V. Kovchegov, D. Pitonyak, and M. D. Sievert, J. High Energy Phys. 10 (2017) 198.
[44] A. Adare *et al.* (PHENIX Collaboration), Phys. Rev. D **90**, 012007 (2014).
[45] G. Bunce, N. Saito, J. Soffer, and W. Vogelsang, Annu. Rev. Nucl. Part. Sci. **50**, 525 (2000).
[46] A. Airapetian *et al.* (HERMES Collaboration), J. High Energy Phys. 06 (2008) 066.
[47] J. Dudek *et al.*, Eur. Phys. J. A **48**, 187 (2012).
[48] R. Akhunzyanov *et al.* (COMPASS Collaboration), Phys. Lett. B **793**, 188 (2019); **800**, 135129(E) (2020).
[49] L. Adamczyk *et al.* (STAR Collaboration), Phys. Lett. B **719**, 62 (2013).
[50] C. Ewerz, M. Maniatis, and O. Nachtmann, Ann. Phys. (Amsterdam) **342**, 31 (2014).
[51] C. Ewerz, P. Lebiedowicz, O. Nachtmann, and A. Szczurek, Phys. Lett. B **763**, 382 (2016).

[52] P. Lebiedowicz, O. Nachtmann, and A. Szczurek, Phys. Rev. D **94**, 034017 (2016).
[53] D. Britzger, C. Ewerz, S. Glazov, O. Nachtmann, and S. Schmitt, Phys. Rev. D **100**, 114007 (2019).
[54] A. Donnachie and P. V. Landshoff, Phys. Lett. B **296**, 227 (1992).
[55] P. A. Zyla *et al.* (Particle Data Group), Prog. Theor. Exp. Phys. **2020**, 083C01 (2020).
[56] A. Karch, E. Katz, D. T. Son, and M. A. Stephanov, Phys. Rev. D **74**, 015005 (2006).
[57] R. C. Brower, J. Polchinski, M. J. Strassler, and C.-I. Tan, J. High Energy Phys. 12 (2007) 005.
[58] L. Cornalba and M. S. Costa, Phys. Rev. D **78**, 096010 (2008).
[59] S. K. Domokos, J. A. Harvey, and N. Mann, Phys. Rev. D **80**, 126015 (2009).
[60] R. C. Brower, M. Djuric, I. Sarcevic, and C.-I. Tan, J. High Energy Phys. 11 (2010) 051.
[61] M. S. Costa and M. Djuric, Phys. Rev. D **86**, 016009 (2012).
[62] M. S. Costa, M. Djurić, and N. Evans, J. High Energy Phys. 09 (2013) 084.
[63] A. Amorim, M. S. Costa, and M. Järvinen, J. High Energy Phys. 07 (2021) 065.
[64] S. J. Brodsky and I. A. Schmidt, Phys. Lett. B **234**, 144 (1990).
[65] S. J. Brodsky, M. Burkardt, and I. Schmidt, Nucl. Phys. **B441**, 197 (1995).
[66] E. S. Ageev *et al.* (COMPASS Collaboration), Phys. Lett. B **633**, 25 (2006).
[67] C. Adolph *et al.* (COMPASS Collaboration), Eur. Phys. J. C **77**, 209 (2017).
[68] C. Adolph *et al.* (COMPASS Collaboration), Phys. Rev. D **87**, 052018 (2013).
[69] B. Adeva *et al.* (Spin Muon Collaboration), Phys. Rev. D **70**, 012002 (2004).
[70] A. Airapetian *et al.* (HERMES Collaboration), J. High Energy Phys. 08 (2010) 130.
[71] N. Sato, W. Melnitchouk, S. E. Kuhn, J. J. Ethier, and A. Accardi (Jefferson Lab Angular Momentum Collaboration), Phys. Rev. D **93**, 074005 (2016).
[72] P. Chen and X. Ji, Phys. Lett. B **660**, 193 (2008).
[73] M. Hirai, S. Kumano, and N. Saito (Asymmetry Analysis Collaboration), Phys. Rev. D **69**, 054021 (2004).
[74] C. Bourrely and J. Soffer, Phys. Lett. B **740**, 168 (2015).
[75] S. Xu, C. Mondal, X. Zhao, Y. Li, and J. P. Vary, arXiv: 2209.08584.
[76] A. Bacchetta, F. G. Celiberto, M. Radici, and P. Taels, Eur. Phys. J. C **80**, 733 (2020).
[77] Y. Zhou, N. Sato, and W. Melnitchouk (Jefferson Lab Angular Momentum Collaboration), Phys. Rev. D **105**, 074022 (2022).
[78] R. Abdul Khalek *et al.*, Nucl. Phys. **A1026**, 122447 (2022).
[79] X.-D. Ji, W. Melnitchouk, and X. Song, Phys. Rev. D **56**, 5511 (1997).
[80] S. Scopetta and V. Vento, Eur. Phys. J. A **16**, 527 (2003).
[81] S. Boffi, B. Pasquini, and M. Traini, Nucl. Phys. **B649**, 243 (2003).
[82] S. Boffi, B. Pasquini, and M. Traini, Nucl. Phys. **B680**, 147 (2004).
[83] A. Vega, I. Schmidt, T. Gutsche, and V. E. Lyubovitskij, Phys. Rev. D **83**, 036001 (2011).
[84] D. Chakrabarti and C. Mondal, Phys. Rev. D **88**, 073006 (2013).
[85] C. Mondal and D. Chakrabarti, Eur. Phys. J. C **75**, 261 (2015).
[86] D. Chakrabarti and C. Mondal, Phys. Rev. D **92**, 074012 (2015).
[87] C. Mondal, Eur. Phys. J. C **77**, 640 (2017).
[88] S. Xu, C. Mondal, J. Lan, X. Zhao, Y. Li, and J. P. Vary (BLFQ Collaboration), Phys. Rev. D **104**, 094036 (2021).
[89] B. Kriesten, P. Velie, E. Yeats, F. Y. Lopez, and S. Liuti, Phys. Rev. D **105**, 056022 (2022).
[90] D. P. Anderle *et al.*, Front. Phys. **16**, 64701 (2021).
[91] E.-C. Aschenauer, S. Fazio, K. Kumericki, and D. Mueller, J. High Energy Phys. 09 (2013) 093.
[92] M. Burkardt, Int. J. Mod. Phys. A **18**, 173 (2003).
[93] M. Burkardt, Phys. Rev. D **62**, 071503 (2000); **66**, 119903 (E) (2002).
[94] R. Dupre, M. Guidal, and M. Vanderhaeghen, Phys. Rev. D **95**, 011501 (2017).
[95] S. J. Brodsky and G. F. de Teramond, MDPI Phys. **4**, 633 (2022).